2015
Summer

BIU-YU
Abstract Book

The BIU-YU Summmer Research Internship

The BIU-YU Summer Science Research Internship program offers a unique opportunity for select undergraduates, primarily from Yeshiva College and Stern College along with appropriate students from other universities, to participate in research in one of the state-of-the-art Bar-Ilan laboratories. Since its inception in 2011, the program has benefited from the generosity of Dr. Mordecai D. Katz, Chairman of the Bar-Ilan Board of Trustees, who has supported the YU student participants, and the J. Samuel Harwit Z"L and Manya Harwit-Aviv Charitable Trust. The program enables talented undergraduates to be exposed to and contribute to Israeli science by working alongside one of Bar-Ilan's more than 180 distinguished science and engineering faculty members. Herein are summaries of the Summer 2015 efforts.

Program Directror:
Prof. Ari Zivotofsky

Av & Em Bayit:
Rav Eliav and Adi

Table of Contents

Chemistry & Physics

Engineering & Computer Science

Life Sciences

Neuroscience & Psychology

Editors:

Joshua Blau

Aviva Cantor

Emily Chase

Yael Steinberg

Layout & Design:

Elizabeth Farkas

From left to right: Jonathan Karp, Matthew Feinstein, Chaim Metzger, Benjamin Aivazi, Yael Steinberg

Improving the Resolution Limit of the Bonding Energy of Ultracool Li7 Atoms

Benjamin Aivazi

Advised under Dr. Lev Khaykovich

One of the ways to trap and cool atoms is through the use of a Zeeman slower and a magneto-optical trap. The particular slower that we used employs lasers and magnetic fields to cool a cloud of Lithium7 atoms to the order of a few μK, with a spatial spread of approximately 200 microns. Under these conditions, the lithium atoms can form weakly bound dimers that can be studied. To more accurately measure the binding energy required for such interactions, we needed to install a more uniform magnetic field. We designed and implemented a Helmholtz-like coil to introduce such a field, and tested it under various conditions prior to installing it on the system. We determined how our particular coil combination would react to changes in frequency and capacitance, which would allow for simpler modification of the field if necessary. The field created was significantly more uniform and provided us with better results than before. When analyzing the data resulting from conducting the experiments with the slower, there was a shift in the resonant frequency when extrapolating it from the number of atoms present versus the magnetic field, which was expected. The sources of this shift are known, and we were able to account for it. We are in the process of running more trials and gathering more data before we can analyze it and determine the new resolution limit of the binding energy of the dimers, which will then aid us in further studies in the field.

Fabrication of Organic Distributed Feedback Lasers Via Soft Lithography

Matthew Feinstein

Advised under Dr. Yaakov Tischler

A laser is a device which produces “coherent light,” which means that the emitted light waves are of the same frequency and have a constant phase difference. Lasers consist of a gain medium which, when excited by either electricity or another laser, emits light of a specific wavelength. Additionally, there must be some optical feedback mechanism, typically mirrors, that keeps the light contained in the gain medium so that the light can be repeatedly amplified.

I was tasked with the fabrication of organic distributed feedback (DFB) lasers. In an organic laser, organic dyes serve as the gain medium. Organic dyes can be cheap to produce, and can be synthesized into a wide array of dyes with specific properties. A DFB laser is characterized by a diffraction grating that provides the optical feedback by utilizing Bragg reflections. The diffraction grating can be described as an ordered series of hills and valleys, with a specific periodicity that only reflects a desired waveband back towards the gain medium. For our target of red laser light

(~620 nm), we needed to have a grating with a peak-to-peak distance of ~417 nm.

Figure 1.

Figure 1a and 1b: Epoxy Copy of an 1800/mm Grating (periodicity of 555.6 nm) Measured Using Atomic Force Microscopy

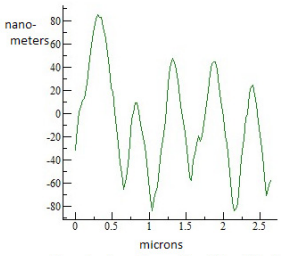

Figure 1a shows the profile of the diffraction grating. The x-axis represents movement along a line perpendicular to the grating lines, while the y-axis represents corresponding change in the height

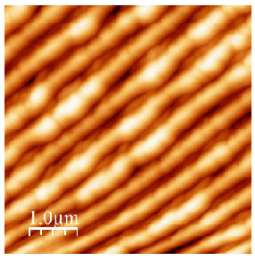

Figure 1b shows an overhead view of the diffraction grating. The AFM software renders taller, "closer" features as lighter colors, and deeper, "further" features as darker colors. This provides asense of the topography

The manufacture of nanoscale patterns like this can be expensive and inefficient. Such gratings can be made using electron-beam lithography or photo-lithographic techniques, but this requires expensive equipment. I worked on producing these gratings using methods of “soft lithography,” which is cheaper and more efficient. The technique I used involves the use of polymers that create a negative image of an original grating. This negative image, the master mold, is then used to stamp a different polymer and create a positive image of the grating. One master mold can be used to create many copies of the original grating, and these copies can be coated with organic dyes to create laser devices. This method of soft lithography also allows the creation of very thin laser devices made of flexible plastic. In theory, minute flexing of this thin laser film should create noticeable shifts in the lasing wavelength, which could have an array of applications, such as sensor technology.

Figure 2.

Figure 2a and 2b: Original ThorLabs 1800/mm Grating (Periodicity of 555.6 nm) Measured Using Atomic Force Microscopy

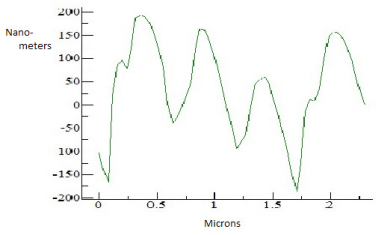

Figure 2a shows the profile of the grating. The periodicity of ~555 nm is visible.

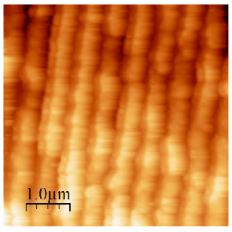

Figure 2b shows the overhead mapping of the grating.

The most finely detailed grating I copied with adequate success has a peak-to-peak distance of ~555 nm. See Figure 1 for an atomic force microscopy scan of the copy and Figure 2 for that of the original.

Divergence of time averaged PDFs in Semiclassical Dynamics

Jonathan Karp

Advised under Dr. Emanuele Dalla Torre

In this project we consider the dynamics of quantum systems with many bodies. We employ a semiclassical approximation in which classical equations of motion are used to study the time evolution. In physics, any system is completely described by the position and momentum of each particle. In quantum mechanics, the position and momentum are not scalars but they are described by complex wavefunctions that are related to probability distribution functions (PDFs). In semiclassical dynamics, we look at an ensemble of equivalent systems with different initial conditions, treat those different initial conditions as a PDF, and solve the dynamics of the system using classical equations of motion.

Figure 1.

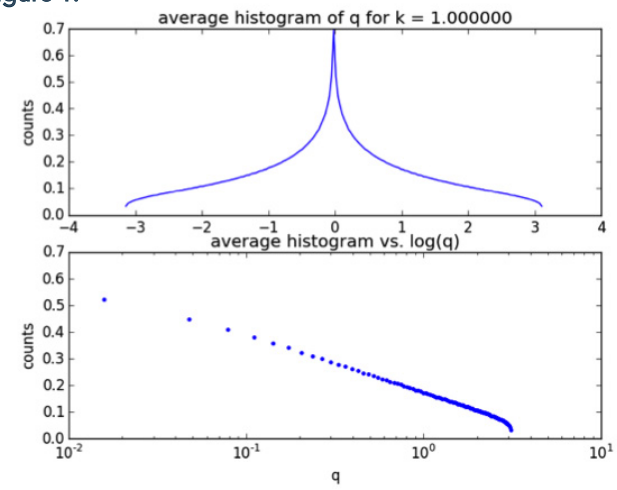

Figure 2.

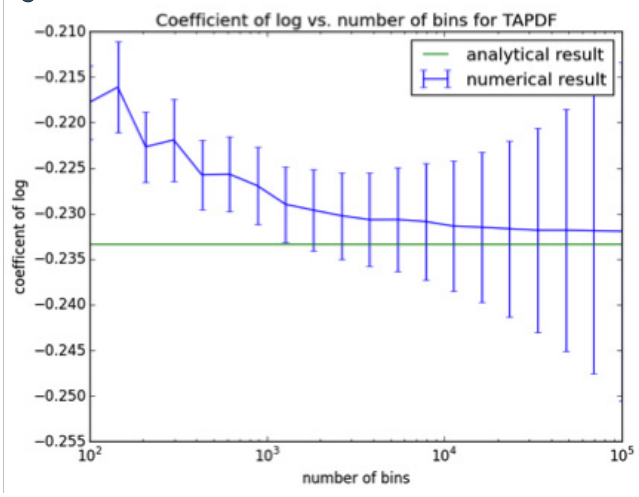

I used this technique first for a simple pendulum with Hamiltonian $H= 1/2*p^2 - k*\cos(q)$ with the momentum initially 0 and the initial displacement distributed uniformly over the region [-π, π]. The time average PDF (TA-PDF) of the system shows logarithmic divergence at q = 0 (Figure 1). Both the fact that the divergence is logarithmic and the coefficient of the logarithm can be found analytically by using the linear approximation of the system. The numerical result approaches the analytical result as the number of bins approaches infinity, and with a sufficient number of bins the numerical result agrees with the analytical result within the error bars (Figure 2).

I next used this technique for a system of two pendulums coupled by a spring. The Hamiltonian of this system is given by :

$$H = \frac{p_1^2}{2m} - k_1 sin(q_1) + \frac{p_2^2}{2m} - k_2 sin(q_2) - \alpha sin(q1 - q2)$$

For high values of relative to k1-k2 the TA-PDF of q1 is non-analytic at 0 and appears to be linear near 0. An analytical result for the TA-PDF can then be found by using a quadratic approximation for the Hamiltonian and finding the corresponding TA-PDF. The approximation is valid for values of q1 close to 0 (Figure 3).

Figure 3.

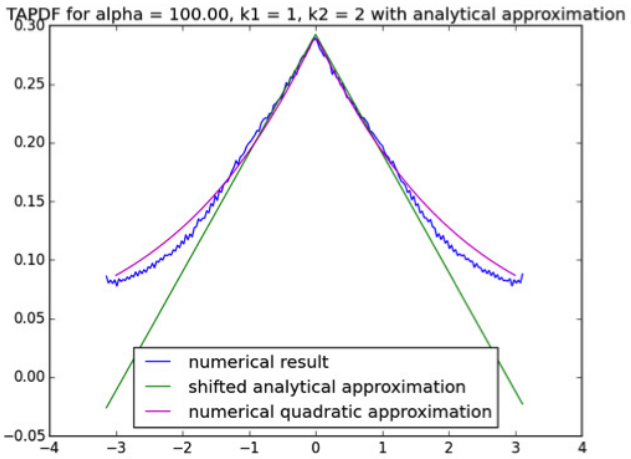

Anomaly in the Anomalous Hall Effect

Chaim Metzger

Advised under Prof. Amos Sharoni

Perpendicular Magnetization Anisotropy (PMA) is the magnetic effect where the preferred magnetization (the easy axis) of a ferromagnetic (FM) thin film is perpendicular to the film. PMA is useful for magnetic memory, as it is more stable than isotropic FM and allows for smaller domains, thus increasing memory density.

> Ferromagnets- are materials that remain magnetic even without an external magnetic field, up to a critical temperature known as the Curie temperature.
> A Paramagnet- is only magnetic in the presence of a magnetic field.

Through the layering of different metals, magnetization can be forced out of plane. We placed a thin layer of ferromagnetic cobalt, a magnetic material, between two 3 nanometer layers of platinum, a nonmagnetic material. By coupling the magnetic cobalt and nonmagnetic platinum, we aimed to get a stronger PMA ferromagnet. The question is how much cobalt is needed in order to make the sample ferromagnetic. We can measure the magnetization through the Anomalous Hall Effect (AHE), which is similar to the Ordinary Hall Effect but with a quantum origin where the electron's spin governs the scattering of the electrons.

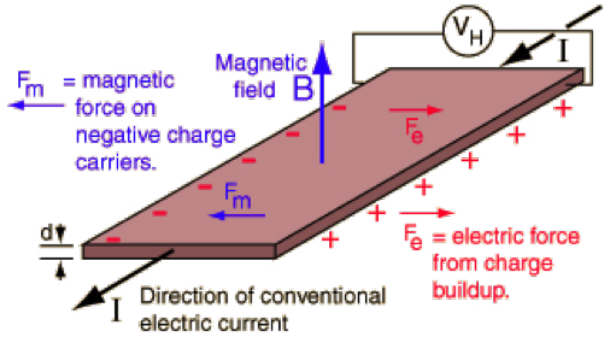

Figure 1. Depicted above is the Ordinary Hall Effect with voltage difference caused by current running through a conductor in the presence of an electrical field. http://hyperphysics.phy-astr.gsu.edu/hbase/magnetic/hall.html

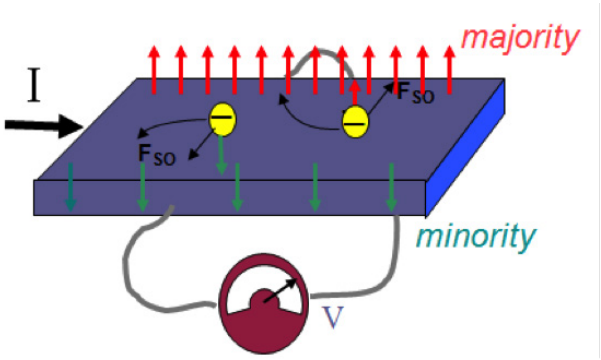

Figure 2. Diagram shows the AHE. Because of the sample's ferromagnetism a majority of the electrons are spin up and tend towards one side of the sample, causing a voltage difference.

We measured the magnetoresistance versus temperature as well as the external magnetic field in order to see how the thickness of the cobalt layer controls the magnetic properties of the sample. We found that from 0.2 nm to 0.5 nm the Curie Temperature (the temperature at which the sample ceases to be ferromagnetic) changed drastically, even increasing to above room temperature in some samples. The Curie temperature changed from 75K to 225K based on different thickness from 0.15 nm to 0.3 nm, to over 300K for 0.5 nm. This shows a difference of 100k for just one monolayer of the material.

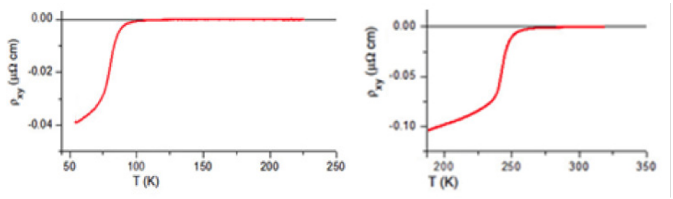

Figure 3. AHE for samples with Cobalt thickness of 1.5Å and 3Å as function of temperature.

To better view the AHE we cooled the sample with no present magnetic field, so that the only contribution we see is from AHE and not OHE. We found an anomaly to the AHE only for the 0.3 nm thickness where there is an unexpected increase in the AHE signal at low temperatures (below 40k) [Figure 3] which does not correspond with the magnetization, the origin of which still needs to be determined.

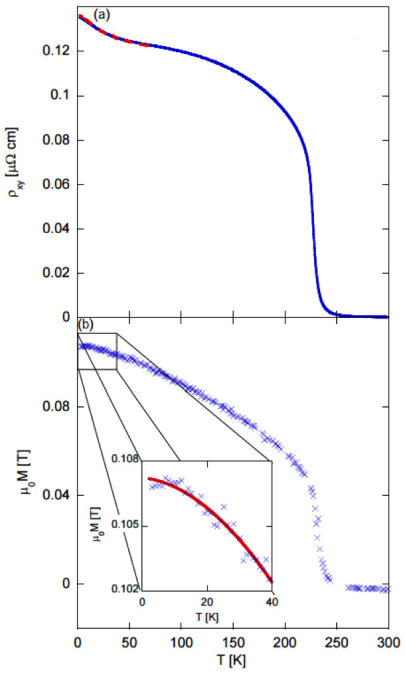

Figure 4. (a) AHE resistivity (ρxy) as a function of temperature. (b) Perpendicular component of magnetization (M⊥) as a function of temperature. Inset focuses on 0 to 40K

Formation of BSA Microspheres by Ultrasonic Cavitation and Investigation of their Chiral Interactions

Yael Steinberg
Advised under Prof. Aharon Gedenken

The laboratory of Professor Aharon Gedenken focuses on the field of Sonochemistry. The laboratory utilizes ultrasound waves for fabricating new materials for applications that include antibaterials, bio-imaging, and catalysis.

My research work focused on one step sonochemical formation of BSA microspheres and their chiral interaction with several amino acids. In this work, we examined the interactions between these microspheres and racemic mixture of amino acid. We began the experiment by creating BSA microspheres using BSA aq. solution and Dodecane. After formation of BSA microsphere, 10 mL of microspheres were added to 10 mL of each DL amino acid solution. These mixtures were placed inside dialysis bags for dialysis of the unreacted enantiomer in water. Samples were taken every 24 hours.

The samples were tested using a Circular Dichroism Spectrometer (CD). This analysis confirmed that there are some enantiomeric interaction between the aq. solution of racemic mixture and BSA microsphere. We are still in the process of processing our data, but early results have been promising.

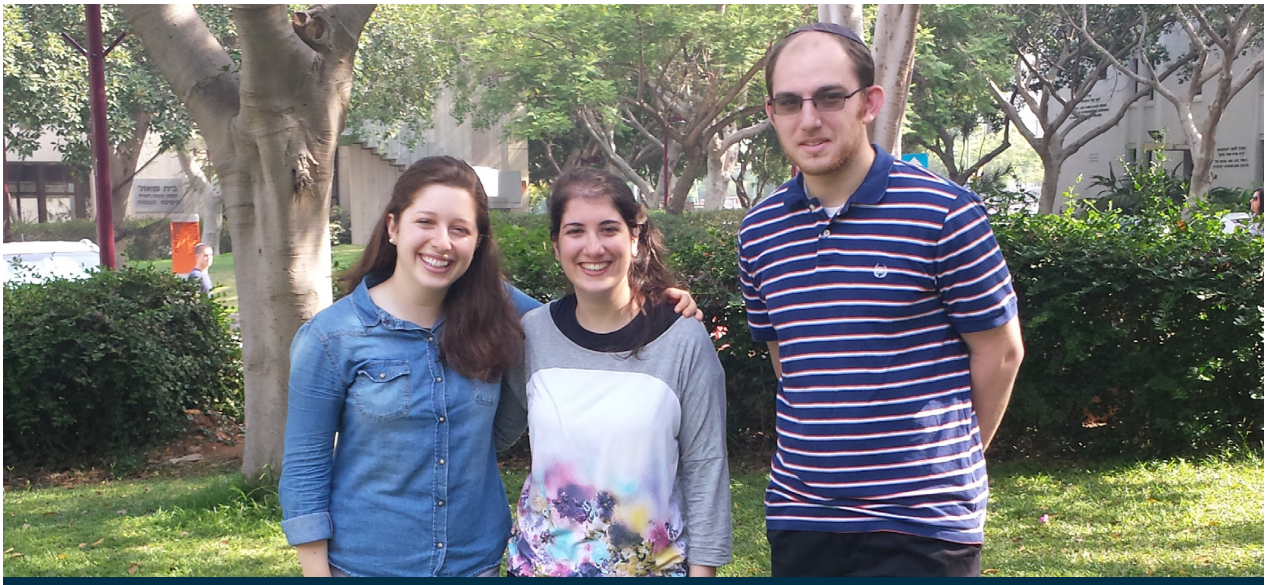

From left to right: Malka Katz, Elisheva Elbaz, Natan Bienstock

Hide and Seek: Designing Intelligent Recommendation Agents to Maximize Platforms' Profits

Natan Bienstock
Advised under Prof. David Sarne

When people buy airline tickets, they usually believe that they have bought their ticket at the best price. When they fly, however, they are often dismayed to discover that the person sitting next to them actually bought the same ticket at a cheaper price. Our research focused on how to ensure that people purchase their tickets at the best price.

Flight price prediction algorithms use historical price data to give predictions of how much flights will cost. For each flight that is examined, the algorithm generates a distribution of expected prices, and based on this prediction makes a recommendation to the user. If the advisor determines that the current price is the best price that the flight will reach, the advisor will recommend that the user buy now. If today's price is not the lowest predicted price, the advisor will recommend waiting until tomorrow and then asking it again.

Our research centered around taking existing flight prediction agents and determining how best to present their predictions to the user to ensure that the user buys now. This research focused on the perspective of the platform, and was concerned with maximizing the platform's profit. The problem from the platform's perspective is that, on the one hand, the platform would like the user to always buy immediately, because the platform does not know if the user will return to their site. On the other hand, if a platform always tells the user to buy, the platform seems dubious, and there is no reason for the user to trust its advice.

We experimented with different methods of presenting the prediction data to the user to ensure that the user buys now more often. We developed a buy or wait game that has ten rounds, and in each round the player is shown a different flight, given advice by an agent, and asked whether to buy now or wait to purchase until tomorrow. This two-day scenario mirrors a situation in which a company might be asked by one of its customers to help solve a problem, and the company only has two days to purchase the ticket. The company needs to know whether to purchase the ticket today or wait until tomorrow in order to achieve the greatest savings for their company.

We are developing four versions of this game in order to determine the best method for the advisor to convince people to purchase most often. In the first version of the game the advisor always recommends to buy now without giving any justification. Figure 1 is a screenshot of a round of this game.

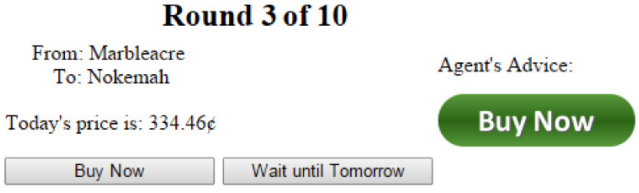

Figure 1: A sample round of the buy/wait game.

In the second version of the game, the advisor will always recommend to buy now, but will also provide the user with a distribution of the price prediction and arguments to convince the user to buy now. In the third version of the game, the agent will occasionally choose to recommend to the user to wait to purchase the ticket, and will then provide the user with arguments as to why the user should wait. In the fourth version of the game, the agent will occasionally decide not to give any recommendation in a situation where it would not benefit the user to buy now, and will instead just provide the user with the price distribution and arguments about the data.

We hope to continue this research into two related, yet different directions. The first is to determine how to present the agent's advice in a way that will maximize the user's savings. The second is to discover how to give the advice in a manner that will give the user the most satisfaction with his/her purchase.

Tumor Detection Via Gold Nanoparticles

Elisheva Elbaz

Advised under Dr. Dror Fixler

Early detection of cancer is crucial for effective treatment. Currently CT scans are used to detect tumors but they are inexact. Gold Nanoparticles (GNP) coated with EGFR are being researched to detect cancer. They are favorable for a few reasons. GNPs are non-toxic, they have desirable optical properties and are less expensive and less invasive than CT scans.

Slides of human mouth tissue were examined with a hyper spectral microscope. The microscope shined wavelengths of light from 450 to 950 nm on each tissue to obtain their absorbance spectra. Then GNPs were added to the tissue and the spectra were again obtained. The two spectra for each tissue were compares to each other to extract the spectrum for the GNPs. A small amount of the particles bind to healthy cells, but since they are coated with EGFR, they are targeted for tumor cells and bind there in great numbers.

Each sized nanoparticle has different optical properties and a different peak. If the graph of the obtained spectrum has a peak at the expected value, it means that a significant amount of GNP binded to the cells and it is likely a tumor.

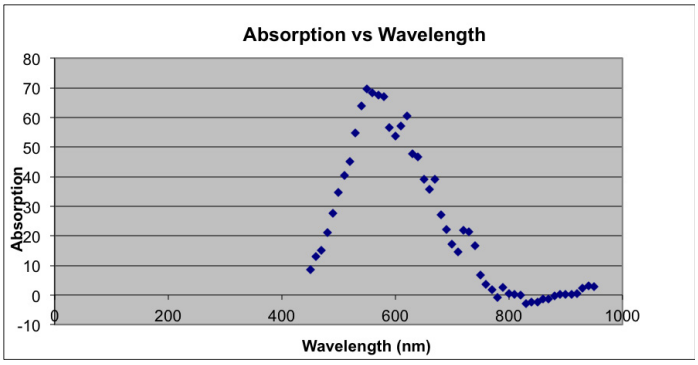

Figure 1. GNPs absorbance spectrum captured by the hyper spectral microscopy, and obtained by subtracting the spectrum of the tissue with and without GNPs. The peak is 550 nm which is the expected peak for the GNPs that were used.

Using nanoparticles to detect tumors can be very useful. Aside from being easier than the technology used now, it can be more exact. The exact borders of the tumors can be determined and this can enable the tumor to be completely removed.

The Effect of Metallic Nanoparticles on Neuronal Growth and Differentiation

Michelle (Malka) Katz

Advised under Dr. Orit Shefi, in collaboration with M.Sc student Michal Marcus

Nerve regeneration following tissue injury or disease is a major challenge in the neuroscience field. The search for regenerative agents that promote neuronal growth and repair is of great interest. Different molecules and materials have been shown to induce and affect neurite outgrowth and elongation. Previous experimentation has shown that iron oxide nanoparticles (NPs) promote neuronal growth and differentiation. Our study tested whether different metallic NPs (gold and silver) would promote significant neuronal growth and differentiation as well as the iron oxide NPs shown to have promoted.

For experimental purposes, PC12 cells were utilized as the neuronal model. PC12 cells, derived from a pheochromocytoma (neurodocrine tumor) on a rat's adrenal medulla, serve as a common model for neuronal differentiation. In response to nerve growth factor (NGF), PC12 cells differentiate into neuron-like cells and outgrow neurites. In our project we incubated the metallic nanoparticles with PC12 cells and studied their effect on the cells' growth and differentiation process. Nanoparticles of all metals had a diameter of 20nm.

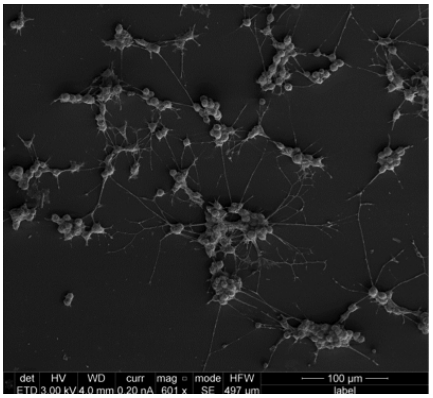

Figure 1. Neurites outgrowth by PC12 cells plated on collagen coated plates, following NGF treatment with addition of metallic nanoparticles. Images were taken by scanning electron microscope (SEM).

First, gold and silver nanoparticles at different concentrations were tested for their toxicities through an XTT assay, thereby determining their cell viability in the PC12 cells. The gold NPs had an insignificant toxicity effect and proved viable for the PC12 cells to uptake; the silver NPs, however, were found to be toxic to the cells.

Next, the cells' morphology was studied along their differentiation processes. The experiment composed of capturing images and measuring the neuronal growth of PC12 cells seeded on collagen-coated plates under a light microscope over the course of seven days (days 1, 3 and 7). The growth of PC12 cells was compared based on the different composites of particles added. We measured and analyzed the neurites using the NeuronJ Program, finding that there was a significant increase in the length of neurites of cells treated with the gold NPs than of neurites of the untreated cells.

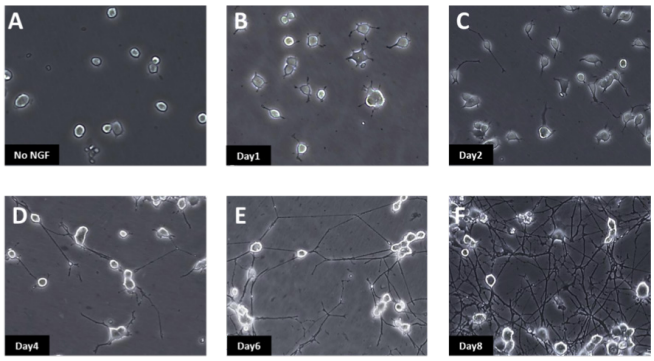

Figure 2. Neurites outgrowth by PC12 cells plated on collagen coated plates, following NGF treatment. (A) Unexposed to NGF. (B - F) Treated with NGF (50 ng/ml) for 1, 2, 4, 6 and 8 days, respectively. Images were taken by light microscope (Magnification: 20x).

Our research contributes to the field of neuronal repair, hoping to benefit pharmacological pursuits in the application and treatment of neurodegenerative diseases, such as Parkinson's, Alzheimer's and Cerebral Palsy.

Top row from left to right: Akiva Abramowitz, Sruli Farkas, Jonathan Falk
Bottom row from left to right: Julie Bree, Devorah Natelson, Merav Gold, Batsheva Reich, Ariella Levie, Emily Chase, Elizabeth Farkas, Rebecca Van Bemmelen

MEIG1 Effect on B-Lymphocyte Development

Akiva Abramowitz
Advised under Prof. Jeremy (Rami) Don

Meiosis, the fundamental evolutionarily conserved differentiative process by which haploid gametes are produced, is complex and tightly regulated. Of the many number of genes that are expressed during mammalian gametogenesis, the murine meiosis expressed gene 1 (MEIG1), was identified as a key component in meiosis, abundantly expressed in both male and female mice. The MEIG1 protein found in mice is also evolutionarily conserved in humans; the MEIG1 gene found in humans is eighty seven percent identical to the MEIG1 gene found in mice.

Dr. Don's Laboratory has observed that MEIG1 plays an important role in the execution of meiosis in spermatocytes. Mice without the MEIG1 gene, called knock out (KO) mice or MEIG1-null mice, are completely infertile, and the very few seemingly mature sperm cells that could be found in their testis are damaged and immotile. Therefore, MEIG1 seems to be important for the DNA rearrangement process that takes place during meiosis (meiotic recombination).

The lab's working hypothesis is that MEIG1 gene also plays a role in the function of the lymphatic system, specifically within the maturation of the B-cell lymphocytes. B-cell lymphocytes mature within bone marrow. They undergo a DNA rearrangement process, called VDJ recombination, and display an ordered expression of genes and cell surface markers. To examine the possible involvement of MEIG1 in B-lymphocyte development, bone marrow cells of wild type and knockout mice without the MEIG1 protein were compared.

To follow the effect of MEIG1's presence during lymphocytic maturation, B-lymphocytes were separated using antibodies against various markers. Using fluorescence-activated cell sorting (FACS), B-lymphocytes were first separated from bone marrow cells using fluorescently labeled antibodies against CD19 marker. To differentiate between Pre-B cells from immature B cells, CD25 and IgM markers were used to detect the stage in development. If both markers were negative, VDJ recombination did not occur and these lymphocytes were still in the Pro-B stage of development. If CD25 was present but IgM was absent, the lymphocytes were Pre-B cells, but if CD25 was deficient and IgM was present, the B-lymphocytes had passed the BCR checkpoint and the lymphocytes present were more differentiated immature B cells. To observe the effects of the MEIG1 protein in the development of B-lymphocytes, the percentages of lymphocytes in the KO and WT mice present in each stage were compared using the markers mentioned above.

Despite the evidence that suggests the involvement of MEIG1 in

DNA rearrangement processes, the results collected from FACS did not show any significant changes in the percent of lymphocytes in the sub-populations characterizing the differentiated stages of B cells during the two trials of this experiment. When the experiment is repeated, conclusive data may be recorded.

Influence of Exercise-Related Energy Metabolites on Neurogenesis

Elizabeth Farkas
Advised under Dr. Eitan Okun in collaboration with M.Sc student Aviva Rotter-Maskowitz

Adult neurogenesis is the process through which stem cells and progenitor cells proliferate, differentiate, migrate and integrate into an existing neural network. Until the 1990's it was generally accepted that neurogenesis only occurred during pre-natal development and ceased once born. While this is true for the bulk of neural pathways, research in the past 15 years has shown that adult mammalian neurogenesis occurs primarily in two regions of the brain: the subventricular zone and the hippocampus. This exciting discovery has spurred researchers to explore a range of topics including the molecular basis of neurogenesis, the neuronal involvement in learning and memory, neurodegenerative disorders (such as Alzheimer's Disease and Parkinson's Disease), and the recovery from trauma and stroke.

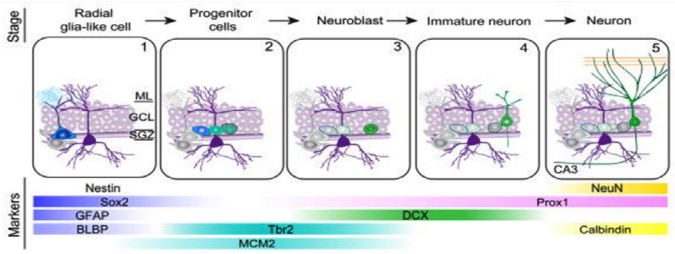

Figure 1. Schematic of neurogenesis processes in adult hippocampus with markers used for immunostaining at each respective stage.

The subgranular zone of the dentate gyrus, a portion of the hippocampus, is particularly notable for contributing to adult neurogenesis. Each day, it produces thousands of cells which set out to become neurons. Very few of those cells actually reach the mature neuron state, with this final number varying depending on factors such as sleep, stress, age and exercise. Among others, these factors determine how conducive the microenvironment is for neurogenesis at any given time.

Aerobic exercise in particular has been shown to have a positive effect on hippocampal neurogenesis. This can be explained by the production of various metabolites that are byproducts of aerobic (and anaerobic) glucose metabolism. The proliferation of neural stem cells and neural progenitor cells are heavily affected by the availability of energetic sources in the brain.

The aim of this experiment is to examine the relationship between an increase in exercise-related energy sources and neurogenesis. To achieve this, *in-vivo* research was conducted, in which the test group of mice was treated with energetic metabolites. After which, a process of immunostaining, image acquisition, and stereological analysis was conducted to quantify neurogenesis. While the lab is presently in the process of stereological analyzation, early results seem promising.

The Effect of Nitric Oxide on Feeding Behaviors in Aplysia

Julie Bree
Advised under Prof. Avy Susswein

Neurobiology often uses animals' simplistic structures to understand more complex ones. Aplysia, a type of marine gastropod, are especially suitable for neurobiology research for this reason. Their large neurons are easy to study and their entire nervous system contains only a few hundred neurons, a tiny number compared to humans' one hundred billion. Despite their simplicity, aplysia have been shown to exhibit a wide variety of behaviors and the ability to learn and retain information. Aplysia research has advanced our knowledge in understanding the biological basis of learning and memory. The focus of my research has been on the feeding behavior of aplysia.

Aplysia spend a great deal of time eating and mating. When they are denied access to food, the extra time is used for mating, causing them to mate almost 50% of the time. This is because feeding and mating are competitive behaviors: when food is available, animals will eat at the expense of mating. It has been found that although feeding inhibits mating, mating excites feeding through pheromones.

Aplysia devote approximately 25% of their time to eating and can eat up to 15% of their body weight in seaweed. Based on this, it would be expected that aplysia naturally eat in large quantities. However, it has been found that when in a "steady state," with constant access to food, aplysia in fact eat very little.

One of the regulators of learning and memory in aplysia is nitric

oxide (NO). It has been found that NO also plays a large part in regulating and inhibiting food intake. The two neurons that have a major role in controlling eating inhibit themselves by releasing NO. L-arginine, the precursor to NO, increases when animals eat, thereby inhibiting eating. This occurs mostly when animals are in a steady state.

My experiments involved combining the inhibitory effect of L-arginine with the excitatory effect of pheromones. Animals in a steady state were injected with arginine and placed in a tank with two mating pairs. Their eating behavior was then compared with those in similar conditions, but not injected with arginine. At first, the results were found to be significant, with the study group eating 40% more than the control group. However, this effect was not upheld in continuing studies.

In the next step of the study, we examined the effects of L-name, a NO inhibitor. By injecting the study group with L-name, we were able to study the combined effects of suppressing the production of NO and exposing the aplysia to pheromones produced by the mating pair. These results have not yet been analyzed.

Difference in Gene Expression in Parental and Transformed Epithelial Cells

Emily Chase

Advised under Dr. Ofir Hakim in collaboration with Dr. Michal Schwartz

Altered gene expression is one of the major causes of carcinogenesis. Expression is commonly controlled by the binding of transcription factors to regulatory sites, which are likely to be found a few hundred kilobases around the gene. The goal of this study was to find transcription factors relevant to the altered gene expression by comparing changes in gene expression with changes in the activity of regulatory regions found in close proximity to the genes of interest. In order to accomplish this, we first had to quantitate the changes in gene expression. We performed RNA-seq on parental and transformed epithelial cells in order to measure the difference in RNA levels. To validate the RNA-seq results, we picked a number of differentially expressed genes and tested them in real-time PCR. Using exon-exon primers to measure total mature RNA, we found that the fold change calculated from the RNA-seq correlated with the data from real-time PCR. The results from both data sets indicate that the genes CDH1, FN1, and LAMC2 are repressed and the genes IL6, PPARG, FGF2, and EGLN3 are activated in cancer-induced epithelial cells when compared with normal epithelial cells. Samples were run in electrophoresis gel following real-time PCR and the results confirmed the identities of the amplified DNA sequences as the intended genes. Biological repeats were performed and results were consistent with previous data. Using intron-exon with real-time PCR to measure nascent RNA, we found that nascent RNA correlate with changes in mature RNA levels determined in RNA-seq, thus showing that most of the changes we see in total mature RNA levels are due to transcriptional changes. The validation of the changes in gene expression after transformation will be used to compare to changes in the activity of regulatory sites in order to identify regulatory sites that are associated with differentially expressed genes. From this data, we aim to determine transcription factors relevant to the changes in gene expression in transformation-induced cells.

Increasing Spatial Resolution of Numerical Models for Land and Air Surface Temperature

Jonathan Falk

Advised under Prof. Steve Brenner and Dr. Itamar Lensky

Air surface temperature (AST) and land surface temperature (LST) influence many areas of life. AST is the temperature that we feel on a day to day basis, while LST is the temperature of the actual surface of the Earth. LST is the dominating factor in determining AST, because the radiation given off by the Earth controls the temperature of the air close to its surface. LST and AST also impact many vital fields, including weather prediction and agriculture. Improving our ability to predict AST and LST on a much finer scale will help make these fields more efficient.

The most accurate and precise way to measure AST is to go outside and use a thermometer. However, it is nearly impossible to measure the temperature at every single point on Earth. In order to make a precise forecast, temperatures at thousands of locations need to be known. Satellites, on the other hand, allow for the entire surface of the Earth to be covered and measured with relative ease. The Moderate-Resolution Imaging Spectrodiameter (MODIS), an instrument aboard the TERRA satellite, orbits and images the Earth twice a day. The LST is

calculated from these images at a resolution of 1 km2, and AST can then be calculated from LST. LST and AST can also be predicted using numerical weather prediction models. However, these models have a much coarser spatial resolution than the satellite (25 km2) , complicating matters where temperature changes drastically over short distances, especially in locations where temperature is driven by local effects.

The method we developed combines the predictive ability of the model with the fine resolution of the satellite in order to create a predictive model at the fine scale resolution of the satellite. This will improve accuracy in forecasting capabilities with regards to AST and LST.

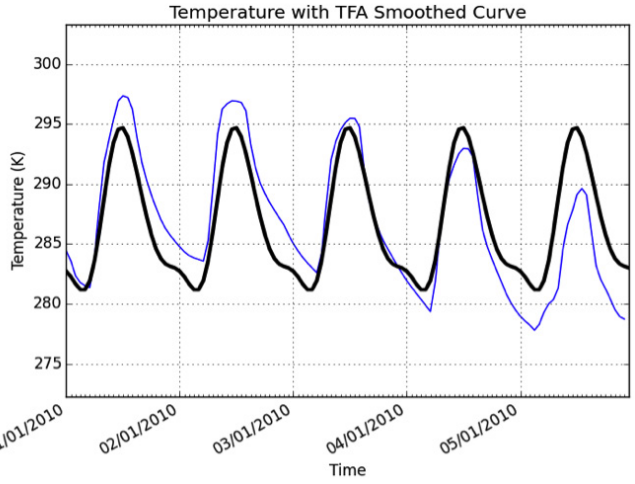

Figure 1. The air surface temperature (blue) with the Temporal Fourier Analysis smoothed curve (black) over a period of 5 days. Temperature is measured in Kelvin.

We used temporal fourier analysis to produce this enhanced prediction, incorporating both the model and the satellite data to create a time series of temperatures. The “noise” was then removed from the time series and a smoothed regular (mean) curve, which is regarded as the climatology or the “expected” temperature (see black curve in Figure 1), was returned. This “noise” is what is commonly referred to as the weather, the difference between the actual temperature (blue curve) and what should be expected for that time of year. The smoothed curve (black curve) was then subtracted from the actual temperature (blue curve), leaving the anomaly (see Figure 2). The anomaly for the model data was calculated and added to the smoothed curve of the satellite data for every point. This yielded the predicted temperature for specific days and times. These values can be used even though the satellite data is not current, as the smoothed curve of the satellite is the “expected” temperature for that time of year and does not change on an annual basis, because it is controlled by synoptic scale patterns, which remains generally constant year to year.

To test our predictive method, the produced temperature will be verified with the actual measured temperature. If the two temperatures line up well, this method could be used to produce a finer resolution than the model with the same or even better predictive capabilities.

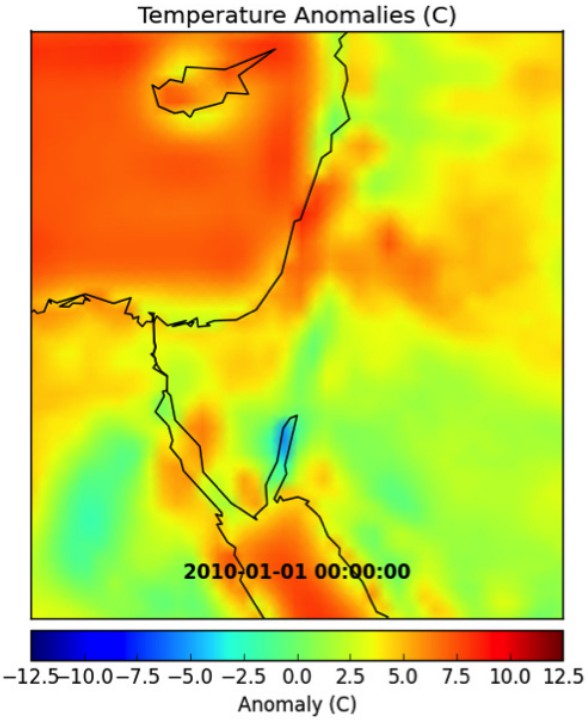

Figure 2. The air surface temperature anomalies for the Eastern Mediterranean coast, calculated from the numerical model. The positive (hotter than normal) anomalies are in red, and the negative (cooler than normal) anomalies are in blue.

Using CRISPR/CAS 9 To Knockout SNF5 in HEK 293 Cells

Merav Gold

Advised under Dr. Achia Urbach in collaboration with M.Sc student Naomi Bollag

The ability to modify a gene in the genome is vital for genetic manipulation and genomic engineering and can be essential in the study of disease. Rhabdoid Tumor, a very rare but fatal pediatric cancer predominantly found in the kidneys, is characterized by a mutation in the gene SNF5, which will then code for non-functional proteins. In this project, we used the CRISPR/ Cas 9 system to knock out SNF5 in Human Embryonic Kidney cells in order to create a model for studying the Rhabdoid Tumor. The

CRISPR system is based on the defense mechanism of bacteria against invading viruses. This system works by creating a double strand break at a specific location using a Cas9 nuclease. The cell's attempt at repairing the break is not precise, so mutations at the site of the break are common. The mutation can cause a "frame shift" if one or two nucleotides are added. This frame shift can cause an early stop codon in the reading frame of the gene, which will cause the protein to be expressed improperly (i.e. a knockout). The result of the knockout and its effects were the first step in creating a model for the Rhabdoid Tumor. There are three levels at which to analyze the effect of the knockout on SNF5: protein, functional, and genomic.

The process of analyzing the effect of the knockout in the HEK 293 cells began by growing clones of the original knocked out cells. In total, 7 clones were grown. Once there were distinct clones, a Western Blot was run to analyze the protein levels in each clone to determine if the frame shift mutation occurred. In clone 7, SNF5 did not appear, implying that a knockout occurred (Figure 1). Since the knockout of a gene can potentially have fatal effects on a cell in culture, an MTS Proliferation Assay was run on samples from each of the 7 clones in order to establish that the HEK 293 cells would continue to proliferate and to test the rate of proliferation, even in the absence of SNF5. The result shows that compared to the wild type, HEK 293 cells with SNF5 knockout will proliferate at a normal rate. (Figure 2).

In order to create a model for the Rhabdoid Tumor based on the SNF5 knockout both the type of mutation and the number of alleles on which it occurs must be determined. Since both alleles cut by SNF5 aren't repaired the same way, mutations can be on one or both alleles and might be different on each allele.

In order to determine the mutation and sequence on each specific allele, the DNA fragments containing the SNF5 gene (either mutant or wild type depending on the clone) were ligated into a T-vector plasmid. Each plasmid can only take up one fragment of DNA, and each competent bacterium can only take up one plasmid, thus ensuring that each sample sent for sequencing is in fact one clean allele. The result of the sequencing showed that clone 7 contains a point mutation, an insertion of A/T (Figure 3), which ruins the reading frame of SNF5, causing an early stop codon (Figure 4). This explains the blank Western Blot for clone 7. This analysis is the first step in creating a model of Rhabdoid Tumor.

Figure 1.

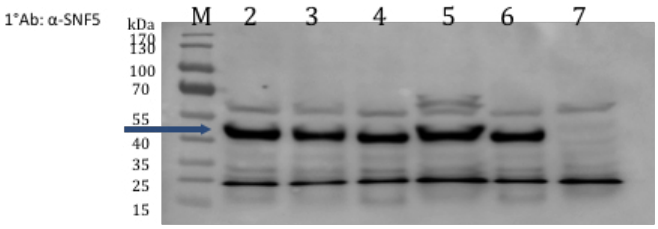

Figure 2.

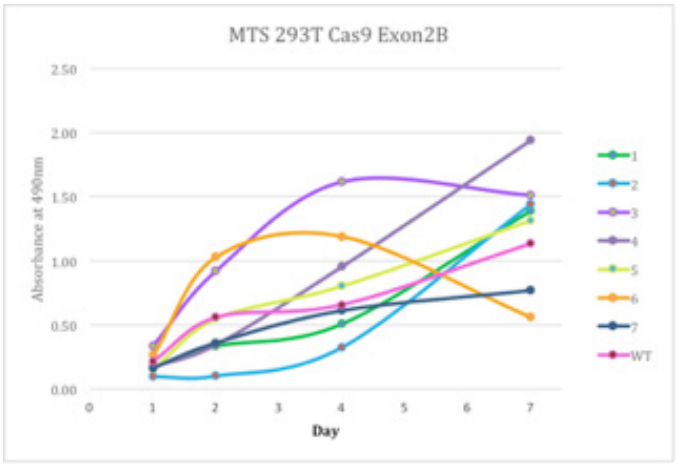

Figure 3. WT top, KO bottom

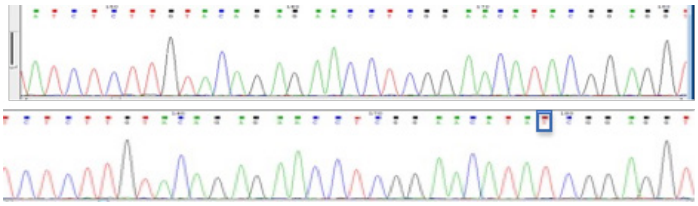

Figure 4. WT top, KO bottom

The SIRT6 Protein and the Molecular Mechanisms of Aging

Ariella Levie

Advised under Prof. Haim Cohen in collaboration with Liat Nehemia

The Sir2 histone deacetylase is a protein that regulates genomic stability and aging in yeast. Researchers have found that this protein is not only found in yeast, but is also found in mammals. There are currently seven known mammalian homologs, SIRT1-SIRT7, that serve the similar function of suppressing genomic instability and increasing longevity. A majority of related research has been done specifically on the SIRT6 protein, which seems to

have the greatest impact on mammalian lifespan. Past research has proven that there is a direct connection between the amount of SIRT6 protein in the cell and the lifespan of the cell. Absence of the SIRT6 protein in mice has been linked to developmental abnormalities that resemble age related degenerative diseases causing the mouse to die within two weeks of birth. The main molecular mechanism by which the SIRT6 protein works is by the removal of the acetylation that appears on many aging proteins. This allows the proteins, and thus the cells, to function normally and live to their fullest capacity. These studies prompted the lab of Professor Haim Cohen to further research the protein in order to elucidate the specific molecular pathways by which the SIRT6 protein is able to increase genomic stability through deacetylation. The key to finding the molecular pathway of the SIRT6 protein is to find out with which other proteins the SIRT6 protein directly interacts. If all proteins which actively associate with the SIRT6 protein are found, it is possible to find the steps of the pathway by which the SIRT6 protein works. The specific process to find all related proteins begins by cloning the SIRT6 gene with a tag into a PGEM plasmid. The SIRT6 gene is then cut out of the PGEM with the enzyme BAMHI and is transferred to PCSC, a viral plasmid. The PCSC is grown in bacteria and the plasmid is then transferred into a virus that infects a 293T cell, a human embryonic kidney cell, making the PCSC with SIRT6 part of the genome of the cell. The cell then grows with the overexpression of the SIRT6 gene, producing large sums of the tagged SIRT6 protein. Cell lysis buffer is then used to extract the proteins from the cell. Immunopercipitation (IP) is used to isolate the SIRT6 protein with the tag. These isolated proteins are run on a Western Blot and transferred to a membrane. Once on the membrane, it is possible to use different antibodies to see which proteins aside from SIRT6 were isolated with the IP method. Any protein extracted along with the SIRT6 must have been directly attached to the SIRT6 protein, which indicates that it interacts with the SIRT6 protein in the deacetylation pathway.

There is one specific disease that it is directly related to human aging. The disease, Hutchinson–Gilford progeria syndrome, is related to the increase acetylation of the lamin A protein. It has been found that in cases where there are decreased levels of SIRT6, the lamin A protein is highly acetylated, leading to its decreased function and an acceleration in aging. In order to find out if the SIRT6 and lamin A proteins are directly related, or related through a long pathway of triggered events, the aforementioned process will be used to see if the lamin A protein gets extracted with the SIRT6 gene.

Evaluation of Animal House Racks by Hormone Extraction

Devorah Natelson
Advised under Dr. Lee Koren

A new animal house was recently built on the Bar Ilan University campus. The University must choose between five brands of racks to purchase for this facility. These racks will hold the cages for the animals housed inside. Differences between racks include the placement of vents (e.g., on top, bottom, side, or completely detached from the racks), which is suspected to play a role in the stress that the animals experience. We are conducting an experiment in order to choose the most appropriate rack based on which model causes the least stress to the animals.

Measuring hair corticosterone, a steroid hormone found in rodents, is one way to assess stress levels. For this study, stress hormone analysis from hair samples is preferable to that of blood samples. Blood samples can show only the hormones that are circulating through the body at the time of sample extraction. In contrast, hair analysis shows the animals' stress levels over a period of time. This is because hormones are deposited into the hair shaft as it grows.

For this experiment, we placed 12 male and 12 female mice in 5 different rack brands, on the top and bottom shelves. Hair was shaved once animals arrived, and 6-8 weeks later. We are extracting hair steroid using methanol, and using commercial enzyme-linked immunosorbent assay (ELISA) kits to measure corticosterone levels in the samples. We will use this data to determine which rack brand induces the least amount of stress in the mice, and therefore which model rack should be purchased for the animal facility.

Effects of Nek1 Knockout on Primary Cilia and on Microtubule Dynamics

Batsheva Reich
Advised Under Dr. Benny Motro

The mammalian NimA-related kinase genes, designated Nek1-11, encode for serine/threonine kinases which are structurally

related to the fungal mitotic regulator, NimA. *Aspergillus nidulans* Never in mitosis A (NimA), is the founding member of the Nek family, and its catalytic activity is critical for initiation of mitosis. Lack of NimA activity leaves fungal cells arrested in G2, where they exhibit interphase microtubules and uncondensed chromosomes. Overexpression of NimA induces a mitosis-like phenotype, includes premature chromatin, condensation, and abnormal mitotic spindles. The NimA-related kinases (Nek's) are generally divided into three major categories. Neks 1, 11, 6, and 2 are involved in DNA damage response. The assembly and length of cilia are affected by Neks 1, 4, and 8. Neks 2, 9, 6, and 7 are related to the cell cycle.

We are currently focused on are Nek1 and Nek7. Nek1 is the largest protein of the mammalian Nek family, consisting of 1258 amino acids. It is known to play a major role in control of the cell cycle, formation and function of primary cilium, and DNA damage control. While overexpression of Nek1 inhibits the formation of primary cilia, cells missing Nek1 appear long and branched or missing altogether. To gain insight into the involvement of Nek1 in primary cilia formation and function, we began analyzing the proteins present and absent in the mutated branch. We ligated Red Fluorescent Protein, RFP, to Centrin, a centrosome protein, which will be used as another tool to mark and identify a sprouting point of the cilia. We also verified different proteins expression to the primary cilia in order to compare protein localization in wild type cells versus mutant cells.

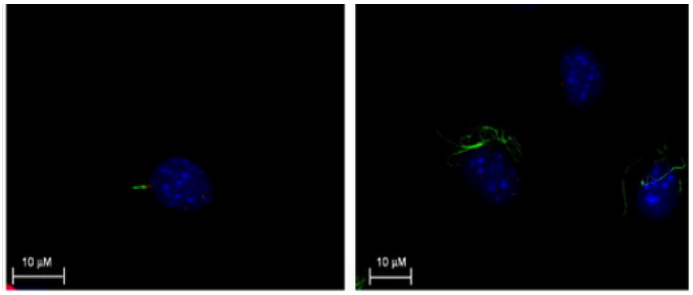

Figure 1. Anti-acetylated-tubulin; Anti-γ-tubuin Hoechst 3342 counterstained nuclei; Shalom et al. 2008

The Nek6/7 subgroup consists of the smallest NimA-Related Kinases, with a core kinase domain and a short N-terminal tail. Nek6 and Nek7 are extremely similar and are highly evolutionarily conserved. There are multiple pieces of evidence indicating a connection between Nek7 and the microtubule network. Nek6 and Nek7 were shown to co-sediment with microtubules. Moreover, these kinases may control spindle formation through phosphorylation of Eg5, a plus-end directed motor protein that cross-links and slides microtubules in an anti-parallel direction, thereby sliding spindle poles apart. Finally, Nek6 and Nek7 are capable of phosphorylating tubulin in vitro. These findings suggest that Nek7 has a direct role in regulation of microtubule dynamics. Our goal was to mark Nek7 with RFP in order to visualize Nek7 together with EB3 and see if Nek7 localizes at the PlusTip end of the microtubule.

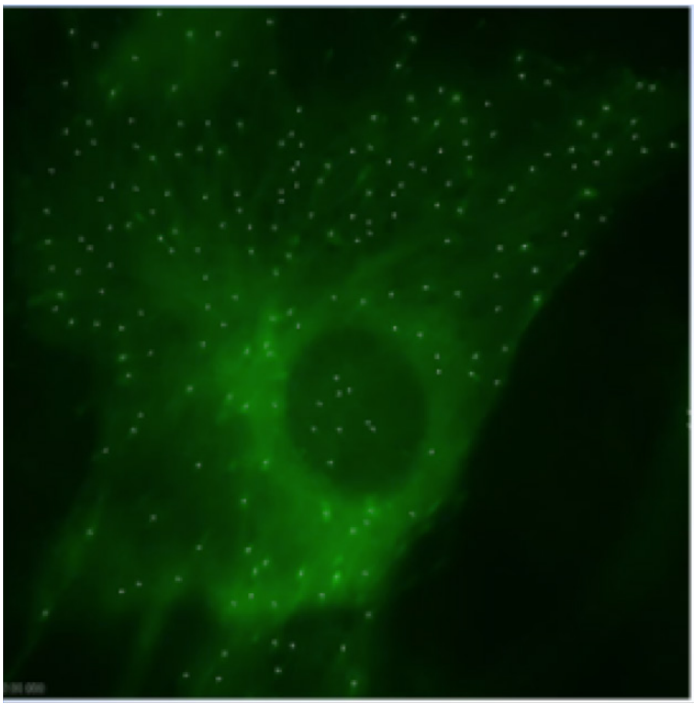

Figure 2. EB3- GFP; Cohen et al. 2014

Development of Neuroligin-2 Mimetics as a Novel Anti-Diabetic Treatment

Rebecca Van Bemmelen
Advised under Dr. Arie-Lev Gruzman

The basis of this research is to develop an anti-diabetic treatment by synthesizing a compound that will cause pancreatic β-cells to increase their production of insulin even if they are under stress conditions. This is because the loss of β -cell functions, specifically the ability to secrete insulin and respond to glucose, plays a major role in the progression of type-2 diabetes. It was recently found that similar to neurons, pancreatic β –cells contain anchor proteins: neuroligins and neurexins on their plasma membrane which help guide 3D intracellual formation and interactions between β –cells. Such proper 3D formation of several β –cells in one conglomerate allows proper production and secretion

of insulin. Among these β –cell proteins, neuroligin-2 (NL-2) and neurexin-1 (NX-1) are the most important ones. Through computer based molecular modeling our lab determined the binding site of the NL-2 to which NX-1 binds, and this nine amino acid peptide (HSA-28) was then synthesized and conjugated to a dendrimer nanoparticle to form the compound HSA-28D (the cluster of HSA-28, Figure 1).

We hypothesized that HSA-28D interacting with a NX-1 on the β-cell-surface would modulate insulin expression and secretion, improve β-cell resistance to cellular stress, prevent apoptosis and increase β-cell mass. To test our hypothesis, we co-cultured the HSA-28D with rat INS-1E cells, which are used as an in-vitro model for β-cell study. The obtained results showed that when cells were co-cultured with varying amounts of HSA-28D, the amount of cells greatly increased. In addition, we determined that with increased cell proliferation, the intracellular level of insulin was significantly elevated in the cells treated by HSA-28D. This was measured by the estimation of the levels of C-peptide (green signal, Figure 2), a component of the insulin precursor which is used as a marker for insulin secretion. Finally, we also found that HSA-28D had a positive effect on the β-cells viability even in the presence of ER and oxidative stressors (Figure 3). We hope that HSA-28D and other NL-2 mimetic compounds will be promising therapeutic agents for diabetes, and that they can be used for creation of stem cell derived artificial islets for future transplantation in diabetic patients.

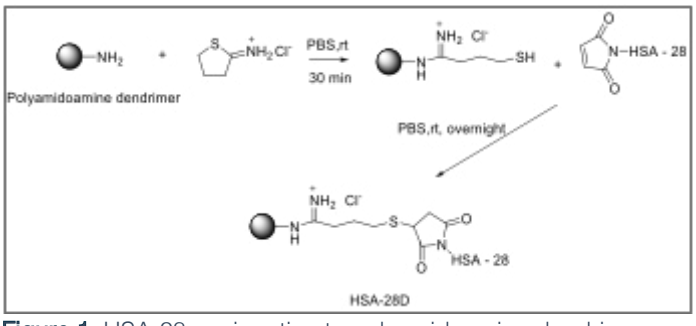

Figure 1. HSA-28 conjugation to polyamidoamine dendrimer (nanoparticle)

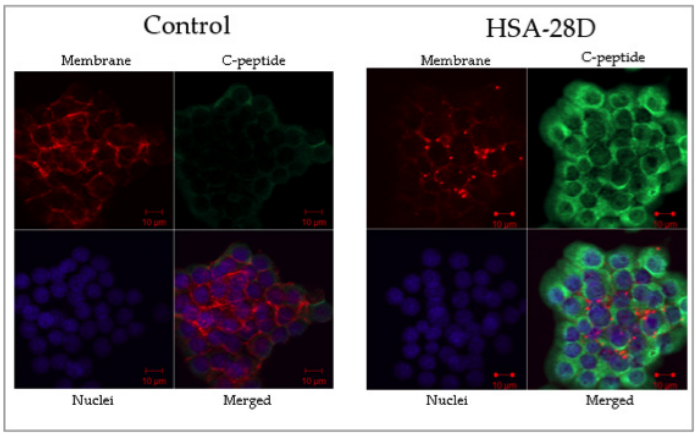

Figure 2. Effect of HSA-28D on C-peptide level in INS-1E cells, visualized using anti C-peptide antibody followed by secondary antibody-green signal

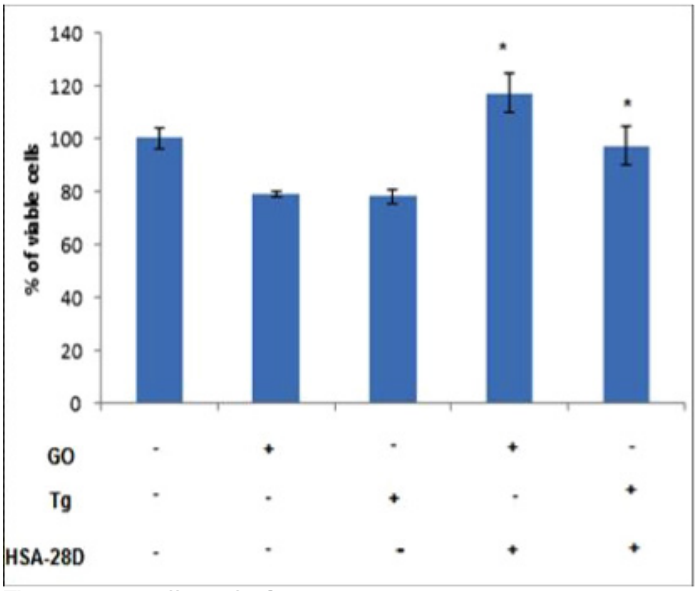

Figure 3. The Effect of HSA-28D on cell viability under oxidative stress and ER conditions

From left to right: Yael Mayer, Aviva Cantor, Elisheva Jakobov, Eliora Habshush, Sara Rozner, Joshua Blau

ISC in MEG in Response to Engaging Videos

Joshua Blau

Advised under Prof. Avi Goldstein

Magnetoencephalography (MEG) is a brain imaging technique that measures brain activity via magnetic fields perpendicular to the surface of the head. Because its data has much higher temporal and spatial resolution than other brain imaging techniques such as functional magnetic resonance imaging (fMRI), it is useful for studying specific frequencies and sections of the brain that may be undetectable using other techniques. Such results are important for cognitive neuroscientific studies, with which my lab is largely concerned.

Functional magnetic resonance imaging (fMRI) studies have found large degrees of inter-subject correlation (ISC) for subjects watching movies in which they were emotionally engaged. However, fMRI is severely limited by the timescale of its hemodynamic responses. MEG, which instead uses neurophysiological imaging, measures brain activity directly, per millisecond over 248 channels, and can pick up much higher frequency signals. Using frequency analysis, this data can be separated into frequency bands, which can then be analyzed individually. For this reason, MEG serves as an excellent platform for testing and narrowing the conclusions of such fMRI studies.

We used short videos (around two and a half minutes) of charismatic speaking and non-charismatic speaking to approximate the effects of the emotional/psychological interest piqued by watching movies, and to serve as stimuli for measuring brain activity with MEG. By analyzing the data in MATLAB, we measured subject correlations in brain activity in alpha, beta, and gamma frequencies, particularly in the surface areas of the brain more relevant to specific frequency bands. After comparing both averaged and individual Fourier transformed timecourses of MEG data against the audio track of the videos by using an enveloping technique, it was clear that the charismatic video had a significant effect on ISC, thus corroborating the fMRI findings. To further solidify these results, the analysis will continue on with source localization.

Effect of Combat Exposure on Emotional Facial Expression Recognition and Processing

Aviva Cantor

Advised under Dr. David Anaki

Exposure to dangerous and deadly situations has been shown to affect veterans in a number of ways. Many develop psychiatric disorders, most commonly posttraumatic stress disorder (PTSD), while others show changes in cognitive and social functioning. The recognition and processing of emotional facial expressions is an important aspect of social functioning that has been examined among military veterans. Theories on emotional facial recognition state that the ability is of evolutionary importance,

since the detection of danger allows one to appropriately respond to and/or avoid threats, which provides a survival advantage. Previous studies have shown that threatening facial expressions, such as anger and fear, are detected more accurately and rapidly, and with minimal attentional investment, as compared to neutral and happy facial expressions. Other facial expression processing studies demonstrate a "negativity bias," in which negatively valenced emotional facial expressions elicit a greater physiological response than positive or neutral emotional facial expressions.

Our study examined how exposure to threatening situations affects emotional facial recognition in combat veterans on a behavioral level, as well as the differences in emotional facial processing of combat and noncombat veterans on an electrophysiological level. Forty-one combat and noncombat veterans of the IDF participated in the study. Questionnaires that measured the presence of PTSD and anxiety disorder were administered before testing, and no significant differences were found between the combat and noncombat groups. Participants of both the combat and noncombat veterans groups were presented with a series of emotional faces (anger, happy, sad, fear, disgust and neutral) and were asked to identify the emotion. It was hypothesized that the combat veterans would show greater recognition of the negative emotions as compared to the non-combat group. Differences in the emotional facial processing of the two groups were expected to be manifested in event-related potential (ERP) waveforms.

The electrophysiological response to the emotional facial expressions was measured using ERPs, the measured brain response that results from the presentation of a specific visual or auditory stimulus. ERPs are measured using electroencephalography (EEG), and serve as a noninvasive means of examining cognitive functioning. The components of the ERP waveform we primarily focused on were the posterior P1 and N170, the frontal N1 and P2, and the LPP. The amplitude and latency of the aforementioned wave components were analyzed using BrainVision Analyzer 2.0. A three-way interaction effect was found for group, hemisphere and emotion. An asymmetry was found in the right and left hemispheres for N170 amplitude corresponding to the processing of emotional facial expressions (Figure 1). Combat veterans showed higher responses in the left hemisphere (P7 and P9 electrodes), while noncombat veterans

Figure 1.

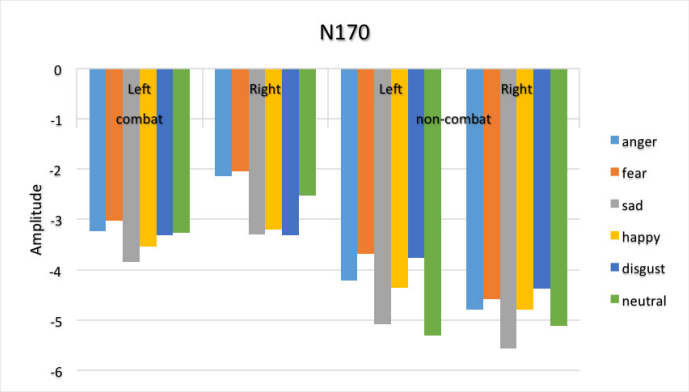

Figure 2.

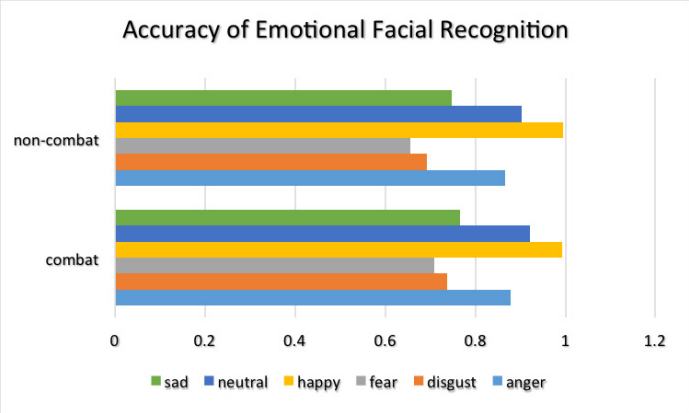

Figure 3. Image of an ERP waveform from the frontal Fz electrode, showing the N1, P2 and LPP components

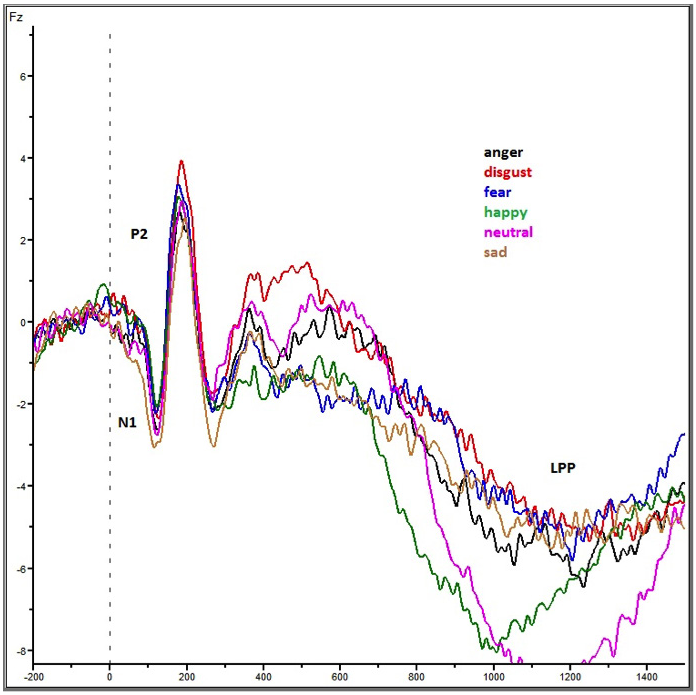

showed greater responses in the right hemisphere (P8 and P10 electrodes).

Accuracy of facial expression recognition was measured as the behavioral component of this study. Our results indicated a significant main effect for emotion. Although both combat and noncombat soldiers identify emotional faces with similar accuracy, they do show a difference in their recognition of fear and disgust expressions, and the emotions themselves vary in terms of the accuracy with which they are recognized (Figure 2). Our findings suggest that there are indeed some differences in the emotional facial expression processing of combat and noncombat veterans.

What Underlies Memorability of Visual Patterns?

Eliora Habshush

Advised under Prof. Msohe Bar

Humans have the ability to remember thousands of images. Despite that fact, all visual information we encounter in life are not equally memorable. It is widely known that there are individual differences in memorability, but it turns out that there are objective factors that contribute to visual memory as well. There are many well known factors that affect visual memory, demonstrated by prior research, such as self-relevance, emotional arousal, meaningfulness, etc. However, there are other factors whose role in visual memory have not been assessed or are still under debate.

In the current study, we aim to estimate the independent relative contribution of different factors that might be relevant to the process of memory. After evaluating the factors, we plan to examine the effects of different learning types (intentional/ incidental) on these processes. Lastly, we are interested in investigating the neural mechanisms that mediate these memory effects.

The first stage of the study involved conducting Stimuli Normalization, which aimed at scaling the different factors that potentially contribute to visual memory. Following, a memory experiment is currently being performed. We plan to analyze results from the factor scaling and examine how the different factors affect visual recognition memory.

During my time spent working at Professor Moshe Bar's lab this summer, I was involved in recruiting and running participants for the memory experiment. Additionally, I began analyzing data from the Stimuli Normalization on SPSS.

The findings of the present study are noteworthy as they indicate that important contributing factors of visual memory can be applicable to many fields. Educators can utilize these results in developing memorable diagrams to illustrate important concepts necessary for students to remember, thereby making learning easier. Advertisers seeking consumers and artists aiming to acquire an audience can also benefit from these findings.

Self-Disclosure of Positive Emotions in Close Relationships of Socially Anxious Individuals

Elisheva Jakobov

Advised under Prof. Eva Gilboa-Schechtman in collaboration with Phd student Noa Choder

The emotional well-being of an individual is dependent on relationships developed and nurtured throughout one's lifetime. Relationships allow for the development of intimacy, which ultimately provides a good support system crucial to a person's emotional hygiene. Social anxiety disorder, also known as social phobia, is a disorder in which individuals experience excessive fear when placed in social and/or performance situations. For socially anxious individuals, close relationships become disrupted easily. These individuals find it difficult to interact with others, and establish and maintain relationships due to the heightened fear of being judged or misrepresenting their true selves. For this reason, socially anxious individuals tend to have fewer close relationships in comparison to non-socially anxious individuals, and also tend to overly rely on these few close relationships. However, even within their close friendships, socially anxious individuals appear to disclose less information regarding their thoughts, emotions, and experiences, thereby decreasing the benefits of intimacy and support they can potentially be receiving from their peers.

The goal of the study was to analyze patterns of self-disclosure focusing on positive experiences and emotions in close relationships of socially anxious individuals. Two separate studies were conducted and participants were asked to write about a positive experience they had within the past month. Prior to each experiment, participants were asked to identify the name of an individual with whom they felt close to, and rate how close they felt to that individual on a scale from 1-5 (not close-very close).

Study 1 (n=292) focused on the association between social anxiety and the tendency to disclose positive emotions and experiences. In this study, participants were requested to write about three different events during which they experienced pride, joy, and closeness. Participants wrote these narratives as if they were writing to a stranger and were then asked to depict the same exact emotional experience, however, this time around they were asked to address their writing to the person whom they previously designated as their close friend.

The goal of study 2 (n=226) was to determine whether patterns of self-disclosure are malleable in socially anxious individuals and whether an increase in self-disclosure is associated with an increase of positive affect in socially anxious individuals. Study two focused on experiences of closeness and joy. Narratives from both studies were then coded for words that are related to emotions and words indicating specificity of experience, including time, location, and duration of said experience. Phase one entailed determining coding criteria and training the coder in applying those criteria to judgments of the narratives. In phase two, the coding was completed and recorded. In the future, additional raters will code the data and interrater reliability will be assessed.

Although analysis of the data is at the very beginning stages, current results indicate that socially anxious individuals tend to use fewer emotional words in comparison to socially non-anxious individuals. Additionally, the analysis of specificity indicates that socially anxious males do not describe their experience in a specific manner. However, with females, this effect was not found. By better understanding patterns of self-disclosure in socially anxious individuals' close relationships, an area which has previously received little attention, possible therapeutic interventions can assist these individuals in establishing stronger, closer and more intimate relationships with others.

Identifying the Early Markers of Autistic Spectrum Disorder and Social Communication Disorder Using Gaze-Tracking and Behavioral Observation

Rebecca London

Advised under Prof. Ronny Geva

Autistic Spectrum Disorder (ASD) and Social Communication Disorder (SCD) are developmental disorders that affect an individual's ability to interact in the social world. ASD and SCD share many characteristics, including abnormal eye contact and gaze patterns, a preference for nonsocial stimuli, and an inability to understand social cues. Although many of these symptoms begin to appear in infancy, an official diagnosis is typically not made until age two or three. This longitudinal study seeks to identify the early markers of ASD and SCD to increase the likelihood of an earlier diagnosis and subsequent interventions.

Three groups of infants are studied. One group with a genetic risk for developing ASD, the second with a developmental risk for ASD, and the third—a yoked-control group. The infants are assessed at nine months and at 18 months. Gaze-tracking paradigms are used to track gaze patterns and eye contact in response to various stimuli. Behavior is also measured through Mother-Infant Social Interaction (MISI), and the Griffiths Language and Personal-Social Scales (GMDS-SF).

During the recorded MISI sessions, the infants' behavior is analyzed and coded based on a number of variables including affect, vocalizations, gaze, eye contact, joint attention, social interaction, behavioral requests, repetitive play, and initiation/reaction in play. Joint attention (JA) occurs when two people focus on a third object, such as a toy or book. Individuals with ASD often have difficulty engaging in JA, and it is therefore a crucial factor in the early identification of ASD. Studying these characteristics in infancy will hopefully lead to earlier, and thus more effective, interventions for young individuals with ASD and SCD.

Learning and Neuronal Pathway as Mediated by Olfactory Stimuli

Yael Mayer

Advised under Dr. Rafi Haddad

Past research has demonstrated a clear relationship between the olfactory system and memory; it has become axiomatically accepted that memory and learning function in tandem as well. Therefore, our objective was to demonstrate a connection between scent and learning, and to subsequently determine the neuronal pathway that processes olfactory stimuli and odor localization.

To test this correlation between scent and learning, our lab used mice in odor discrimination tasks. Mice placed on a water restriction diet had a streams of air shot at randomly chosen sides of the nose, with only the stream shot to the right side of

the nose resulting in a water reward. In measuring performance with unscented or scented air streams, the olfactory system's role is tested. A mouse licking the water tube after perceiving a scent from the right in anticipation of the water reward was marked as a "hit" via a lick sensor. Licks made from the air stream supplied from the left were recorded as a "miss." Percentages were then calculated to determine the learning performances of mice with scented versus unscented air. If significant success rates would indicate that olfactory senses aid the learning process. Owing to the connection between scent and learning, we hypothesized that the mice would perform more successfully when presented with scented air. The unscented air trials thus served as a control ruling out the air stream itself as a causative factor and serving as a baseline of comparative success. The experiment was performed at various air pressures and with different odor concentrations. Air pressure was lowered until a threshold level of success in scented air and failure in unscented air trails was reached. While conclusive results are still pending, we have thus far found that performance in response to scented air does appear to exceed that of unscented air.

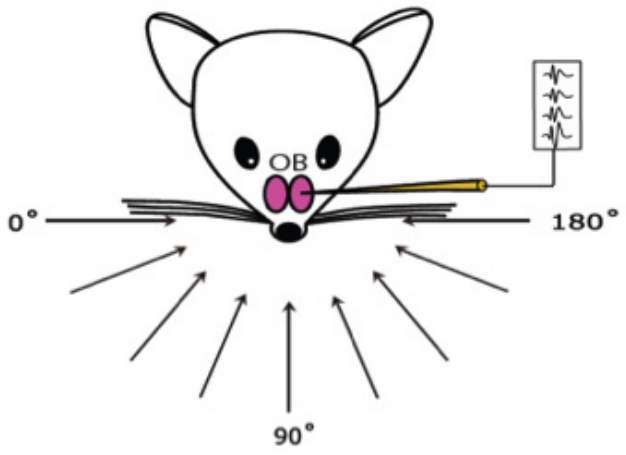

Figure 1. Tetrode in left, contralateral, bilateral, and ipsilateral olfactory stimuli

This finding enabled us to investigate the neuronal pathways and reactions to olfactory stimuli by electrophysical means. With the knowledge that the mice can localize odors, we were able to isolate the right and left olfactory neural pathways. Placing four tetrodes in the left, and subsequently the right, hemispheres of olfactory bulb mitral cells, we recorded the reactions of specific neurons to contralateral, bilateral, and ipsilateral scent air puffs (Fig.1). Neuronal spikes were recorded on a PST histogram (Fig. 2, 3). Although the research is not yet conclusive, our findings showed that some of the neuronal reactions to scent are direction-dependent; certain neurons respond differently to stimuli presented at the right, left, or center of the mice. As such, the neural coding of a given scent presented at the right or left would be significantly different. These findings present the interesting quandary of how the mouse recognizes two different neural codes as the same odor. It is possible that the mouse uses only the consistent, non-direction dependent neurons to determine odor, while they use direction-dependent neurons to determine the direction from which the odor originates.

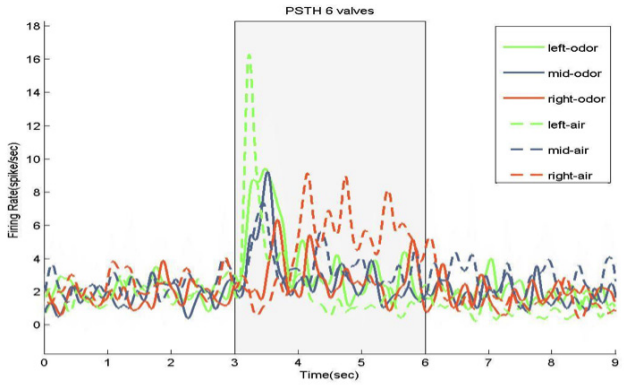

Figure 2. Scent recognition per neuron as measured by neuronal spikes per second

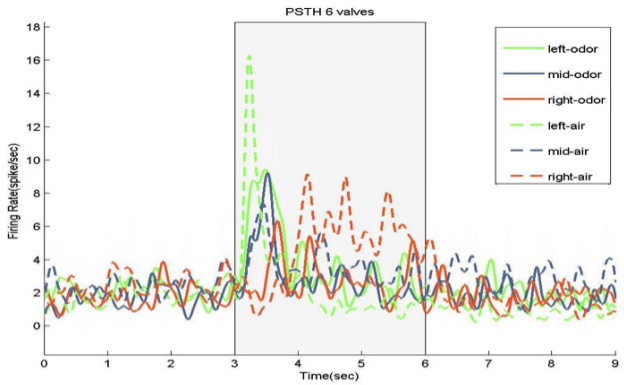

Figure 3. Scent recognition per neuron as measured by neuronal spikes per second

Trait Perception in High and Low Dominant Voices and Faces

Sara Rozner

Advised under Prof. Eva Gilboa-Schechtman

Personality traits tend to be evaluated in clusters, with perceptions of one trait influencing perceptions of related traits. For instance, perception of an individual as attractive would tend to bias other positive trait perceptions, such as intelligence. This cognitive

bias is called the Halo Effect (Thorndike 1920), and has been used to explain correlations between dominance and a variety of positive features, including attractiveness, achievement, and likeability (Zuckerman and Driver 1989). Additionally, although much research has focused on trait perception of faces, these evaluations have been shown to differ from those of both voices and face-voice combinations, which are more representative of real world situations (Peschard et al 2014).

The present study seeks to investigate how dominance in faces, voices, and face-voice combinations effects other trait evaluations, and whether those evaluations are moderated by raters' gender, country of origin, and individual psychological differences such as social anxiety level. Participants (n=147) were recruited from Israel and Belgium, (67 male, 80 female, mean age 27.34, SD = 10.631). In an online study, participants were presented with high and low dominant faces, high and low dominant voices, and stimuli which combined both facial and vocal cues (bimodal) which were either congruent or incongruent in terms of dominance. Participants were asked to rate each stimulus on six traits: attractiveness, friendliness, dominance, intelligence, warmth, and assertiveness.

We predicted that there would be a strong dominance halo effect, with more highly dominant stimuli rated higher in assertiveness, intelligence, and attractiveness, but lower in friendliness and warmth. Additionally, we expected bimodal stimuli to have a higher dominance effect than unimodal stimuli because of the additional information available from two modalities. Our hypothesis was partially supported; dominance was found to have a significant effect on all trait ratings across modalities, including friendliness and warmth, with high dominant stimuli rated higher in all six traits than low dominant stimuli. There were some significant differences in trait rating based on modality, with voices rated higher than faces in handsomeness, friendliness, and warmth. Counter to expectations, bimodal stimuli were rated lower in dominance than faces or voices alone. Although there was no main effect of raters' gender, there was a highly significant effect of country on all trait ratings, with Israelis giving significantly higher trait ratings than Belgians across all traits and modalities.

In a second stage of data analysis, we will seek to investigate whether dominance perception is further moderated by participants' levels of social anxiety. Investigations of Social Anxiety Disorder (SAD) indicate that socially anxious individuals have heightened sensitivity to displays of dominance, and have a lower threshold for dominance perception than not-socially anxious individuals. We predict, then, that participants with higher levels of social anxiety will rate stimuli as higher in dominance than their non-socially anxious counterparts.

Hemispheric roles in semantic and phonological processing in speakers of native and non-native languages

Amalia Schwartz

Advised under Prof. Nira Mashal and Dr. Katy Borodkin

The right hemisphere (RH) of the brain is presumed to have a more central role when acquiring new skills while the left hemisphere (LH) is more critical during the later stages of learning. This can be applied to semantic and phonological processing in a person's native language. According to the Fine vs. Coarse semantic coding theory (Beeman, 1998) the right hemisphere activates a larger range of semantically related words than does the left (Faust & Mashal, 2007). As a result, responses to semantically related words, albeit distantly, are faster and more accurate in the left visual field (LVF)/RH than the right visual field (RVF)/LH. In the current study we test whether the LH plays a more central role for native language (L1) processing, which in this study is Hebrew, while the RH has a dominating role for non-native language (L2) processing, in this case, English.

A previous tachistoscopic study, suggests that speakers process words presented in their native language in the RVF/LH faster and more accurately than words presented to the LVF/RH. However, the opposite is true for non- fluent speakers of a non-native language, suggesting that the RH plays a more important role for secondary language (Karapetsas & Andreou, 2001). Previous research also indicates that Hebrew speakers show no visual field advantage (i.e., bilateral pattern of hemispheric processing) in processing English but do show a RVF/ LH advantage when reading Hebrew. This suggests that there is a division of labor between the two hemispheres based on linguistic experience (Ibrahim, Israeli & Eviatar, 2010).

The present study uses a divided visual field paradigm in order

to examine hemispheric processing of word pairs in Hebrew as L1 and English as L2. Participants in the study will include a sample of native Hebrew speakers who learned English as a secondary language. Participants will undergo two experiments, one in Hebrew and one in English. The stimuli will include 240 word pairs in each experiment in which the target words will be presented to either the RVF or the LVF. The word pairs are either semantically related (ex: sky-cloud), phonologically related (ex: rule-tool), or unrelated (ex: letter-duck). Participants will decide whether the target word is a real word or not (a lexical decision task). In order to construct the stimuli, questionnaires were distributed in order to counterbalance the rate of word frequency and semantic relationships between conditions.

We hypothesized that responses in the native language experiment, which in this case is Hebrew, will be faster in the RVF/LH for phonological conditions and that there will be no hemispheric advantage in the other conditions. However, the opposite is expected in the non-native language experiment. Responses are expected to be slower in the RVF/LH compared to the LVF/RH for phonological conditions. Again, no hemispheric advantage is expected for the semantic processing conditions. This would support the hypothesis that hemispheric involvement in native and non-native language processing depends on linguistic experience. This could suggest that phonologically related pairs are learned separately for each language while semantically related words can be conveyed across languages.